RSC Advances

ROYAL SOCIETY OF CHEMISTRY

www.rsc.org/advances

Journal Name

RSCPublishing

COMMUNICATION

Dynamic electrochemical quantitation of dopamine release from a cell-on-paper system

Cite this: DOI: 10.1039/xoxxoooooox

Raphaël Trouillon[a,]* and Martin A. M. Gijs[a]

Received ooth January 2012,
Accepted ooth January 2012

DOI: 10.1039/xoxxoooooox

www.rsc.org/

A hybrid microfluidic/ electrochemical system is described for the time-resolved detection of dopamine (DA) from neuron-like PC12 cells cultured on a patch of filter paper. Cell adherence to the surface of the paper is investigated using fluorescence microscopy. DA release after stimulation with acetylcholine, in presence or absence of drugs, is studied. Overall, the results obtained with this system are in good agreement with single cell data, thus demonstrating the validity of our approach for higher-throughput quantitative chemical analyses on tissue or organs-on-a-chip.

Neuronal communication is a fundamental physiological event and is usually achieved through exocytosis,[1] where vesicles loaded with neurotransmitters fuse with the cell membrane and release their content in the extracellular space. Important data have been obtained using electrochemistry[2] on addiction,[3–6] exocytotic mechanisms[7–12] or fundamentals of neurotransmission.[13,14] Electrochemical systems are also highly amenable to miniaturization and microfabrication. Implementing electrochemical detection in microfluidic platforms could therefore provide a user-friendly, simple and versatile tool for neuro/ bioanalysis, in addition to more traditional methods.[15,16]

Several perfusion systems aimed at biochemical measurements were described [17–20] where a flow is applied on the surface of the sample (cultured cells or tissue). However, in most of these systems, the cells are grown directly onto the surface of a chip which needs to be regenerated or replaced, which is a tedious process. The relevance of the cell monolayer model is also limited, as some systems require a three-dimensional architecture. Several designs have been suggested to culture cells on-chip in a 3D matrix (typically a gel).[21] A specific strategy has to be determined to load, maintain and cast the gel, and as with the cell monolayer, the chip has to be cleaned and regenerated before use. Finally, fragments of actual tissue, especially slices of excised organs, are a reliable model for biological processes.[22] However, these samples are obtained from animals, thus requiring specific facilities and training, complicating the experimental protocol as well as raising ethical concerns. A cell-based system where the sample can be loaded into the chip, analysed, and easily exchanged would improve the results and the throughput. An easy way to implement 3D cell constructs would also be of considerable benefit for the booming organs-on-a-chip field.[23,24]

Paper has recently attracted a lot of attention as a material for analytical assays.[25–27] Paper is light, cheap, easy to store, handle and process and has been combined to several other techniques,[28] such as electrochemistry,[29,30] wax printing,[31] or enzymatic assays,[32] to address specific analytical problems. Interestingly, it has also been shown that paper could be used as a substrate for cell culture.[25,33] The mechanical strength of paper allows for the easy manipulation of the cell constructs, thus enabling new experimental strategies, such as the stacking of different paper layers. This has been applied for instance to cell chemotaxis under oxygen gradients[34] or ischemia.[35]

Here, we describe a versatile, modular electrochemical/ microfluidic system for the dynamic, time-resolved detection of dopamine (DA) released from PC12 cells upon acetylcholine (ACh) stimulation, as described in Fig. 1A. These cells were grown in a 3D matrix deposited on patches of filter paper,[25,33] which allowed for the easy manipulation and the facile loading of the sample into the chip. In our hands, a single sample could be loaded, tested and removed in ~15 minutes. Importantly, the porous and solid nature of the paper patches allowed us to flow the stimulating buffer across the sample, rather than over its surface. Doing so, the totality of the sample is exposed to the stimulant, and the temporal resolution is increased, even though the delay times due to dead volumes have to be taken into account. The results obtained from our system were all in good agreement with results previously obtained with single cell amperometry, which

requires a much heavier experimental setup. These data also provide, to the best of our knowledge, the first dynamic chemical measurements from cell-on-paper samples. The effect of dynasore, an inhibitor of dynamin which was also reported to inhibit DA exocytosis,[7] was tested and was found to appear more acute than at the single cell level, for similar concentrations. Overall, this study demonstrates the validity of the use of simple, affordable and quantitative analytical devices for the online, real-time and dynamic study of neuro-secretion.

We used standard soft lithography on poly(dimethylsiloxane) (PDMS) to make a simple microfluidic system, composed of two main parts. The sample chamber, where the sample was placed, was made of two identical pieces (Fig. 1A) themselves made of five layers. The design of the sample chamber was inspired from devices previously reported for maintaining pieces of excised tissue.[19,23,22,36] A second component, the detection chamber, made from a single piece of PDMS bound to a glass slide and containing the electrochemical sensor, is placed downstream. The separation of the detection chamber from the sample chamber guarantees easy manipulation of the sample, removal of the bubbles, etc, without compromising the stability of the sensor. The electrochemical part of the system was prepared by threading a Ø 51 µm Pt wire (working electrode WE) and a chloridised Ø 75 µm Ag wire (reference electrode RE), both Teflon coated in the lumen of a 20 G blunt syringe needle, with the needle acting as a counter electrode, CE (Fig. 1B). The sensor was found to follow the general theory of electrochemistry, as shown in the Supporting Information. The idea of integrating the sensor into a syringe needle and using it into a microfluidic system has already been suggested by others.[37–39] The limit of detection for DA was found to be few nM (see Supporting Information). Fabrication protocols and characterisation data of the chip are presented in the Supporting Information.

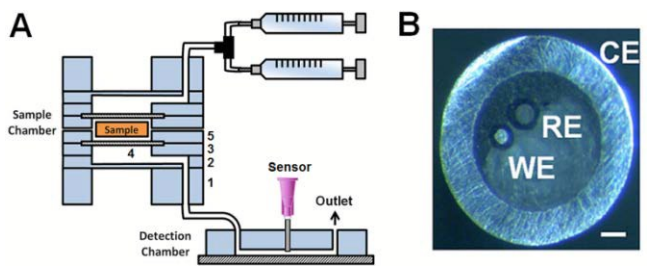

Fig. 1: Description of the system. A- Scheme of the complete device (not to scale), with the input syringes, the sample and detection chambers, and the electrochemical sensor. B- Micrograph of the tip of the needle sensor, showing the three electrodes: working (WE), reference (RE) and counter (CE) electrodes (scale bar: 100 µm).

To prepare the cell-on-paper samples, PC12 cells (European Collection of Cell Cultures) were re-suspended in media at $2x10^8$ cells ml^{-1} and mixed, in a 1:1 ratio, with cold (4˚C) extracellular matrix (ECM) gel from Engelbreth-Holm-Swarm murine sarcoma. A 5 µl drop of the mixture was then spotted on a ~ Ø 5.5 mm patch of Whatman filter paper 114 and incubated for 2-4 hours. The patches were imaged using DAPI to observe the cells and the effect of the flow. On paper alone, (Fig. 2A) a significant level of background of signal can be observed, probably originating from cellulose auto-fluorescence in the near-UV.[40,41] Upon addition of cells, the presence of adherent cells can be clearly observed as grainy structures (Fig. 2B). DAPI is an affordable way of imaging these samples, and the high background was not considered here a major issue.

One of the main concerns was that applying a 1 µl s^{-1} flow for 10 minutes would wash away the cells. To investigate this, some paper patches were exposed to these flow conditions, imaged and compared to control (no flow applied) patches (Fig. 2C). No obvious difference can be observed in cell density or in coverage area. At a higher magnification, random images did not reveal any difference after exposure to hydrodynamic conditions. Furthermore, only a few cells were detected at the bottom of the culture wells, indicating that almost all the seeded cells adhere to the paper patch.

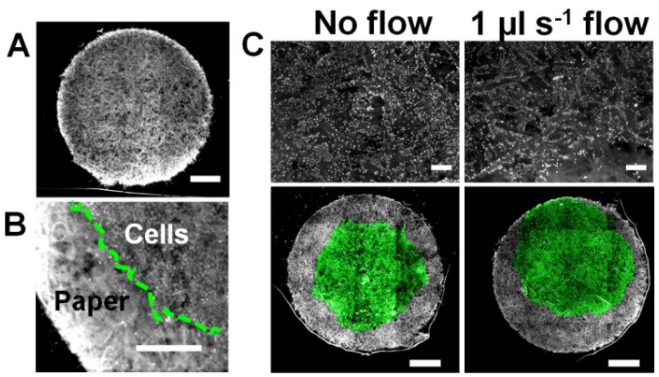

Fig. 2: Imaging of the DAPI-stained cell-on-paper patches. Micrographs at 5x of A- a control paper patch at (scale bar 1 mm) and B- a cell-seeded paper patch, showing the limit between the cell population and the free paper surface (scale bar 500 µm). C- Micrographs at 10x (top, scale bars 100 µm) and 5x (bottom, scale bars 1 mm) of two typical cell-seeded paper patches, one of which was exposed to a 1 µl s^{-1} flow for 10 minutes. In the bottom micrographs, the surface covered by the cells is highlighted in green. This is a false colour which was overlaid on the original image to facilitate the analysis of the picture.

As shown in Fig. 3A, ACh induces DA release in PC12 through initial receptor binding (step 1), subsequent Na^+ and Ca^{2+} influxes (step 2) resulting in an increase in intracellular [Ca^{2+}] (step 3) and DA exocytosis (step 4).[42] For DA detection, a paper patch loaded with cells was placed in the sample chamber, the system was assembled and the WE was poised at 0.7 V *vs.* Ag|AgCl until the recorded signal was stable under continuous HEPES injection (v=1 µl s^{-1}). All the electrochemical tests were performed using an Iviumstat Powerstat (IviumTechnologies, Netherlands). A stream of 100 µM ACh (in HEPES buffer) was then injected at 1 µl s^{-1} and the electrochemical recording was initiated simultaneously. This concentration was chosen because it has been reported to induce a maximal level of exocytosis.[42] Lower concentrations would reduce the amount of released DA, this was not investigated in this study. After 400 s, the ACh flow was stopped, and HEPES buffer was injected at 1 µl s^{-1}. The experiments were carried out at room temperature, and the sampling frequency was 1 Hz. The traces were processed following the procedure described in the Supporting Information and the dead volume time was subtracted from the time axis, so that 0 s corresponds to the time when the ACh stimulating buffer enters the detection chamber. The data are reported here as average ± SD, for n individual measurements.

Two configurations were tested for the control: a paper patch without cells placed in the sample chamber (n= 6) or leaving the chamber empty (n= 3). No difference could be observed between these two cases (p> 0.08 for a Student's t-test), hinting that the paper patch

alone does not influence the signal. These two datasets were pooled (n= 9) to obtain the control trace shown in Fig. 3B. For a patch seeded with 5 x 10^5 cells (Fig. 3C), a clear increase in current, lasting for the duration of the ACh stimulation, before coming back to baseline, can be observed, and is attributed to the release of DA.

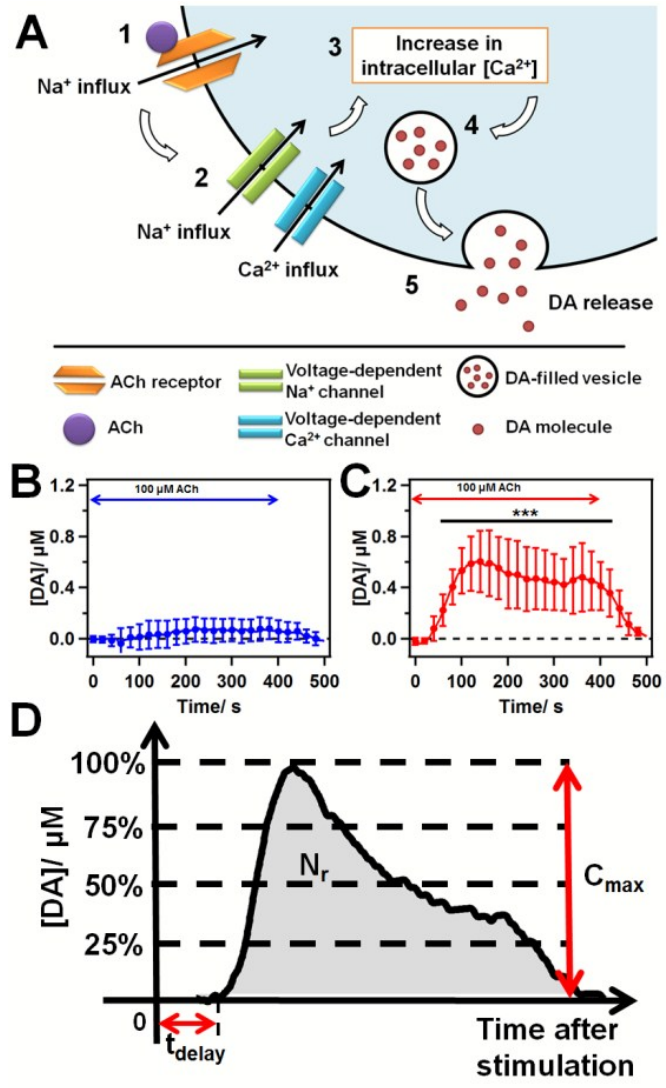

Fig. 3: DA detection. A- Mechanism for DA release after ACh stimulation (see text for details). Results (average ± SD) obtained for the [DA] from B- the control (*i.e.* no cells, n=9) and C- PC12 seeded paper patches (n=7). A two-tailed Student's t-test, assuming equal variances was performed to compare these datasets. On panel C-, the *** symbols indicate p<0.001. D- Parameters (C_{max}, t_{delay}, N_r) obtained from the [DA] traces.

Several parameters were extracted from the individual traces (Fig. 3D). The maximum concentration is C_{max}. The delay time t_{delay} is the time at which the signal exceeds the baseline by 3 standard deviations (SD) of the baseline. Please note that t_{delay}, which is biologically relevant and describes the lag time between the onset of the cell exposure to ACh and the beginning of a detectable DA release, is different from the dead volume time which accounts for a technical parameter and is subtracted during data processing. The area under the curve is multiplied by v and by Avogadro's number to obtain the number of molecules released by the cells, defined as N_r. The average C_{max} was evaluated as 0.62±0.25 µM. Such concentration is not expected to induce sensor fouling from the oxidised DA.[43] This was indeed confirmed by monitoring the variations of the current obtained in a continuous flow of 1 µM DA, as shown in the Supporting Information. The average t_{delay} was 31±7 s. Such a delayed response has already been observed a the single cell level for ACh stimulation,[44] and can be attributed to the slow kinetics of the intracellular cascade leading to DA release (Fig. 3A). Similarly, the average N_r can be evaluated as (11.1 ± 4.7) x 10^{13} molecules. With single cell amperometry, and after a 5-s K^+ stimulation, a PC12 cell typically releases 2x10^6 DA molecules.[45] Assuming a similar level of release over the 400-s stimulation for 500,000 cells, a release of 8 x 10^{13} DA molecules would be expected from the single cell data, assuming that the exocytotic response scales up with the number of cells and the stimulation time. This is in good agreement with our result, which also hints there is no negative cell-to-cell interaction that could decrease the magnitude of the exocytotic bolus. Different stimulants were used for the artificial tissue (ACh) and single cell (K^+) tests, but the amount of DA released per peak was found to be similar at single cells for K^+ and ACh stimulations,[44] thus hinting that the same pool of vesicles is mobilised, which allows for the comparison of these two methods. Hence, the behaviour of PC12 cells is maintained between the different levels (single cell *vs*. population) and the artificial cell/ paper construct quantitatively retains its physiological activity.

L-3,4-dihydroxyphenylalanine (L-DOPA) was used to increase the amount of DA released.[46] A 2-hour long pre-incubation with 100 µM L-DOPA led to a higher C_{max} (1.57 ± 0.19 µM, n= 3, p= 3.3 x 10^{-4} for a Student's t-test) than for the 'no drug' case, in agreement with increased DA release. This results in a ~2.5 times higher N_r after exposure to L-DOPA, (26.2 ± 0.8) x 10^{13} molecules, in very good agreement with the increase observed for single cell data.[45]

Table 1: Comparison of measured and calculated total numbers of released DA molecules N_r obtained from on-chip and single cell measurements, respectively. As detailed in the text, for the single cell data, α_{active} is the proportion of the cell population showing at least one exocytotic spike after stimulation, N_p is the median amount of DA molecules released per exocytotic peak for an active cell, and n_{peak} is the number of peak per active cell. For the single cell data, the theoretical N_r was evaluated using Eq 1.

[Dynasore]/ µM	On-chip			Single cell[a]					
	n[b]	N_r/ molecules	Variation	n[b]	α_{active}	n_{peak}	N_p/ molecules	Theoretical N_r/ molecules	Variation
0	7	11.1 ± 4.7 x 10^{13}	n.a.	23	77 %	30.5	88 x 10^3	8.3 x 10^{13}	n.a.
0.1	4	6.6 ± 2.8 x 10^{13}	-40 %	13	62 %	18.3	74 x 10^3	3.4 x 10^{13}	-59 %
1.0	3	0.0 ± 1.3 x 10^{13}	-99 %	16	60 %	5.9	63 x 10^3	8.9 x 10^{12}	-89 %

a:data published in reference 7.
b: number of patches (on-chip) or cells (single cell) tested.

Dynamin is a GTPase largely involved in endocytosis, which has recently been found to play a strong role in the exocytosis of neurotransmitters.[7] Single cell experiments have found that, if the GTPase activity of dynamin is blocked with the selective inhibitor dynasore,[47] the amount of DA released from PC12 cells is decreased, thus hinting that dynamin facilitates the dilation of the exocytotic pore.[7] To investigate whether this finding translates to tissue-like structures, the DA release from paper patches was measured in presence of 0.1 and 1 µM dynasore. The cells were pre-incubated in the dynasore solution for 5 minutes. The experimental values for N_r are reported in Table 1. As expected, N_r decreased with the concentration of dynasore, for the three cases considered ($p = 5.1 \times 10^{-3}$ for a 1-way ANOVA test). For a concentration of 1 µM, the measured N_r is similar to the one observed for the control 'no cell' case, thus hinting at a complete blocking of the exocytotic activity.

From this dataset, the half maximal inhibitory concentration IC_{50}, *i.e.* the dose needed to obtain 50% of the inhibitory activity, can be evaluated as ~0.1 µM, which is an order of magnitude below the one reported at the single cell level.[7] This can be explained by the different methods used to calculate the IC_{50} in these two cases. For an artificial tissue sample, the total exocytotic activity of the sample is measured directly by evaluating N_r. However, at the single cell level, α_{active}, the fraction of the cell population showing at least one exocytotic spike after stimulation, as a function of [dynasore] was used to evaluate IC_{50}. This criterion does not take into account the eventual reduced median amount of DA released per exocytotic peak, N_p, or the lower number of peaks per active cell, n_{peak}. At the tissue level, all these parameters regulate the amount of DA released, principally as a product of these three values (*vide infra* in Eq. 1). This product simulates better the tissue response and decreases faster with [dynasore], hence simply considering one of these other parameters under-evaluates the blocking effect of dynasore at the tissue level and results in an apparent higher IC_{50}. It is however possible to relate the single cell data to the cell-on-paper measurements, as shown on Table 1. A theoretical N_r can be associated to the single cell data using the following equation:

$$N_r = n_{cells}\alpha_{active}n_{peaks}N_p\frac{t_s(on\text{-}chip)}{t_s(single\ cell)} \quad (1)$$

where n_{cells} is the number of cells on the paper patch and t_s*(on-chip)* and t_s*(single cell)* are the duration of the stimulations (400 s exposure to ACh for the artificial tissue experiment, 5 s K^+ injection for the single cell measurements) for the on-chip and single cell modalities, respectively. As shown in Table 1, in both cases, the measured and theoretical N_r are comparable and lead to similar levels of inhibition. The differences can be explained by minute differences in cell conditions, and the fact that different statistical markers were used (mean for the cells-on-paper tests, median for the single cell experiments). This finding however strengthens the capabilities of tissue-like samples for quantitative assessment of the effects of inhibitors.

The efficacy of a modular microfluidic/ electrochemical system for the dynamic, time-resolved analysis of exocytosis in PC12 cells at the cell population level has been presented and discussed. Importantly, the results obtained for DA release have been found to be in excellent agreement with published data for similar experiments performed at the single cell level. These results provide, to the best of our knowledge, the first example of real-time and quantitative chemical investigation of dynamic mechanisms at artificial cells-on-paper samples. Furthermore, numerous efforts have been recently carried out for obtaining quantitative chemical measurements on single cells.[48–50] Investigating whether these findings also translate at a higher scale in a modular system, in which the cell patches are easily exchangeable, could open the way for higher-throughput dynamic electrochemical measurements in the organ-on-a-chip field.

Funding of this work was provided by the EPFL and the EU Ideas program (ERC-2012-AdG-320404). The authors thank the staff of the CMi at EPFL for assistance in the micro-fabrication processes. The group of Nikolaos Stergiopulos at EPFL is gratefully acknowledged for providing access to its cell culture facility.

Notes and references

a: Laboratory of Microsystems, Ecole Polytechnique Fédérale de Lausanne, CH-1015 Lausanne, Switzerland

* raphael.trouillon@m4x.org

Electronic Supplementary Information (ESI) available: Experimental methods and electrochemical characterisation. See DOI: 10.1039/c000000x/

1 J. E. Heuser, T. S. Reese, M. J. Dennis, Y. Jan, L. Jan and L. Evans, *J. Cell Biol.*, 1979, **81**, 275–300.
2 R. N. Adams, *Anal. Chem.*, 1976, **48**, 1126A–1138A.
3 D. Sulzer, T. K. Chen, Y. Y. Lau, H. Kristensen, S. Rayport and A. Ewing, *J. Neurosci.*, 1995, **15**, 4102–4108.
4 E. C. Berglund, M. A. Makos, J. D. Keighron, N. Phan, M. L. Heien and A. G. Ewing, *ACS Chem. Neurosci*., 2013, **4**, 566–574.
5 E. S. Calipari, M. J. Ferris, C. A. Siciliano and S. R. Jones, *ACS Chem. Neurosci.*, 2015, **6**, 155–162.
6 R. A. Wheeler, B. J. Aragona, K. A. Fuhrmann, J. L. Jones, J. J. Day, F. Cacciapaglia, R. M. Wightman and R. M. Carelli, *Biol. Psychiatry*, 2011, **69**, 1067–1074.
7 R. Trouillon and A. G. Ewing, *Chemphyschem*, 2013, **14**, 2295–2301.
8 R. Trouillon and A. G. Ewing, *Anal. Chem.*, 2013, **85**, 4822–4828.
9 R. Trouillon, Y. Lin, L. J. Mellander, J. D. Keighron and A. G. Ewing, *Anal. Chem.*, 2013, **85**, 6421–6428.
10 L. J. Mellander, R. Trouillon, M. I. Svensson and A. G. Ewing, *Sci. Rep.*, 2012, **2**, 907.
11 L. A. Sombers, H. J. Hanchar, T. L. Colliver, N. Wittenberg, A. Cans, S. Arbault, C. Amatore and A. G. Ewing, *J. Neurosci.*, 2004, **24**, 303–309.
12 C. Amatore, S. Arbault, Y. Bouret, M. Guille, F. Lemaître and Y. Verchier, *Chembiochem*, 2006, **7**, 1998–2003.
13 I. Mitch Taylor, A. Jaquins-Gerstl, S. R. Sesack and A. C. Michael, *J. Neurochem.*, 2012, **122**, 283–294.
14 K. F. Moquin and A. C. Michael, *J. Neurochem.*, 2009, **110**, 1491–1501.
15 S. T. Larsen and R. Taboryski, *Analyst*, 2012, **137**, 5057–5061.
16 J. Wang, R. Trouillon, Y. Lin, M. I. Svensson and A. G. Ewing, *Anal. Chem.*, 2013, **85**, 5600–5608.
17 C. Yamamoto and H. McIlwain, *J. Neurochem.*, 1966, **13**, 1333–1343.
18 H. L. Haas, B. Schaerer and M. Vosmansky, *J. Neurosci. Methods*, 1979, **1**, 323–325.
19 P. M. van Midwoud, G. M. M. Groothuis, M. T. Merema and E. Verpoorte, *Biotechnol. Bioeng.*, 2010, **105**, 184–194.
20 D. S. Weigle, D. J. Koerker and C. J. Goodner, *Am. J. Physiol.*, 1984, **247**, E564–568.
21 S. Chung, R. Sudo, V. Vickerman, I. K. Zervantonakis and R. D. Kamm, *Ann. Biomed. Eng.*, 2010, **38**, 1164–1177.
22 I. A. M. de Graaf, P. Olinga, M. H. de Jager, M. T. Merema, R. de Kanter, E. G. van de Kerkhof and G. M. M. Groothuis, *Nat. Protoc.*, 2010, **5**, 1540–1551.
23 V. Sivagnanam and M. A. M. Gijs, *Chem. Rev.*, 2013, **113**, 3214–3247.
24 S. N. Bhatia and D. E. Ingber, *Nat. Biotechnol.*, 2014, **32**, 760–772.

25 R. Derda, A. Laromaine, A. Mammoto, S. K. Y. Tang, T. Mammoto, D. E. Ingber and G. M. Whitesides, *Proc. Natl. Acad. Sci.*, 2009, **106**, 18457–18462.
26 X. Li, D. R. Ballerini and W. Shen, *Biomicrofluidics*, 2012, **6**, 011301.
27 A. W. Martinez, S. T. Phillips, G. M. Whitesides and E. Carrilho, *Anal. Chem.*, 2010, **82**, 3–10.
28 A. K. Yetisen, M. S. Akram and C. R. Lowe, *Lab. Chip*, 2013, **13**, 2210–2251.
29 W. Dungchai, O. Chailapakul and C. S. Henry, *Anal. Chem.*, 2009, **81**, 5821–5826.
30 Z. Nie, C. A. Nijhuis, J. Gong, X. Chen, A. Kumachev, A. W. Martinez, M. Narovlyansky and G. M. Whitesides, *Lab. Chip*, 2010, **10**, 477–483.
31 E. Carrilho, A. W. Martinez and G. M. Whitesides, *Anal. Chem.*, 2009, **81**, 7091–7095.
32 A. Apilux, Y. Ukita, M. Chikae, O. Chailapakul and Y. Takamura, *Lab. Chip*, 2012, **13**, 126–135.
33 R. Derda, S. K. Y. Tang, A. Laromaine, B. Mosadegh, E. Hong, M. Mwangi, A. Mammoto, D. E. Ingber and G. M. Whitesides, *PLoS ONE*, 2011, **6**, e18940.
34 B. Mosadegh, M. R. Lockett, K. T. Minn, K. A. Simon, K. Gilbert, S. Hillier, D. Newsome, H. Li, A. B. Hall, D. M. Boucher, B. K. Eustace and G. M. Whitesides, *Biomaterials*, 2015, **52**, 262–271.
35 B. Mosadegh, B. E. Dabiri, M. R. Lockett, R. Derda, P. Campbell, K. K. Parker and G. M. Whitesides, *Adv. Healthc. Mater.*, 2014, **3**, 1036–1043.
36 P. M. van Midwoud, M. T. Merema, E. Verpoorte and G. M. M. Groothuis, *Lab. Chip*, 2010, **10**, 2778–2786.
37 B. A. Patel, M. Rogers, T. Wieder, D. O'Hare and M. G. Boutelle, *Biosens. Bioelectron.*, 2011, **26**, 2890–2896.
38 M. L. Rogers, D. Feuerstein, C. L. Leong, M. Takagaki, X. Niu, R. Graf and M. G. Boutelle, *ACS Chem. Neurosci.*, 2013, **4**, 799–807.
39 E. Bitziou, D. O'Hare and B. A. Patel, *Anal. Chem.*, 2008, **80**, 8733–8740.
40 A. S. Blervacq, T. Dubois, J. Dubois and J. Vasseur, *Protoplasma*, 1995, **186**, 163–168.
41 K. H. Malinowska, T. Rind, T. Verdorfer, H. E. Gaub and M. A. Nash, *Anal. Chem.*, 2015.
42 H. Shinohara, F. Wang and S. M. Z. Hossain, *Nat. Protoc.*, 2008, **3**, 1639–1644.
43 W. Harreither, R. Trouillon, P. Poulin, W. Neri, A. G. Ewing and G. Safina, *Anal. Chem.*, 2013, **85**, 7447–7453.
44 S. E. Zerby and A. G. Ewing, *J. Neurochem.*, 1996, **66**, 651–657.
45 R. Trouillon and A. G. Ewing, *ACS Chem. Biol.*, 2014, **9**, 812–820.
46 E. V. Mosharov, A. Borgkvist and D. Sulzer, *Mov. Disord.*, 2015, **30**, 45–53.
47 E. Macia, M. Ehrlich, R. Massol, E. Boucrot, C. Brunner and T. Kirchhausen, *Dev. Cell*, 2006, **10**, 839–850.
48 Y. Lin, R. Trouillon, G. Safina and A. G. Ewing, *Anal. Chem.*, 2011, **83**, 4369–4392.
49 R. Trouillon, M. K. Passarelli, J. Wang, M. E. Kurczy and A. G. Ewing, *Anal. Chem.*, 2013, **85**, 522–542.
50 R. Trouillon, M. I. Svensson, E. C. Berglund, A.-S. Cans and A. G. Ewing, *Electrochimica Acta*, 2012, **84**, 84–95.

For TOC only

A simple hybrid microfluidic/ electrochemical system is used to observe the secretion of neurotransmitters from a cell-on-paper system